Indian Journal of Engineering & Materials Sciences
Vol. 32, February 2025, pp. 146-157
DOI: 10.56042/ijems.v32i01.11872

Acoustic emission response of macro synthetic fibre reinforced concrete beams

Efe Selman*[a] & Gökhan Kılıç[b]

[a]Vocational School, İzmir University of Economics, 35330 Balçova, İzmir, Turkey
[b]Department of Civil Engineering, İzmir University of Economics, 35330 Balçova, İzmir, Turkey

Received: 18 June 2024; accepted: 07 January 2025

Macro synthetic fibre reinforced concrete(MSFRC) has been frequently preferred owing to their adequate ductility, post cracking capacity and toughness values, being potential sustainable alternative material to steel fibre concrete. Their fracture processes and possible failure mechanisms have been simultaneously scrutinized in order to fully exploit from their advantageous structural characteristics. AE methods have accurately provided comprehensive information on the origination and development of a flaw that is located in inner sections of material. With this current study, AE technique has been selected in order to determine the crack evolution and propagation in MSFRC structures. To study the AE response of MSFRC specimens, three MSFRC specimens in the volumetric ratios 0.5%,1% and 1.5% have been prepared and tested with reference concrete specimen. Average frequency, RA(Rise time to Amplitude ratio) and Sentry function parameters have been examined during three-point bending tests for specimens. AE features which correspond to the damage occurrences have been identified and shown during load history. AE method has been found to predict adequately the damage progression of MSFRC elements and the experimental behaviours of specimens have been typically captured well.

Keywords: Acoustic emission, Average frequency, Macro synthetic fibre reinforced concrete, RA, Sentry

1 Introduction

More recently, acoustic emission (AE) techniques have attracted a great deal of attention in the non-destructive testing field. This serious interest arises from the advantages and successful results of AE method. When compared to the other alternative techniques, AE method not only provides real-time results but also offers global monitoring of complex structures scanning the whole structure with a few sensors. The underlying philosophy of AE is the generation of elastic waves due to the deformation and fracture processes within a solid subjected to loading. In other words, AE produced at the source is a pulse of energy that spreads out through the material as an elastic wave because of the development of any flaws or discontinuities in response to loading and stresses. The signal waveforms are easily obtained by using contact sensors and the evaluations are made according to the relevant features of main parameters of AE such as average frequency, amplitude, etc. This principle stated above provides simultaneous and reliable information about the initiation and development of flaws or fractures with the aid of several AE analyses improved. There are various types of analysis based on AE such as parameter analysis, AE-SiGMA, etc. but it is worth noting that they basically rely on the variation in the AE main parameters during increasing stresses and deformations at AE sources[1].

Macro synthetic fibre reinforced concrete(MSFRC) have been essentially developed to provide an alternative to steel fibre reinforced concrete but they offer the structural performances of steel fibre ones owing to the their higher aspect ratios, satisfying strengths and ultimate strain values. The macro synthetic fibres infuse the concrete with higher levels of fracture toughness, energy absorption and ductility. Under increased loading, fracture with matrix cracking, fibre rupture and pull-outs govern the failure mechanism of MSFRC specimen, like in steel fibre reinforced concrete[2-4]. The failure mechanism of MSFRC specimens are generally divided into three stages as regions before the first peak load, between first and second peak load and final failure region after second peak load[5-7]. Under flexural tests, enhanced loading and deformation capacity increased continuously with microcracks occurrences until the first peak load. Around the first peak load main

*Corresponding author
(E-mail: selman@ieu.edu.tr, efe.selman@ieu.edu.tr

flexural midspanmacrocrack forms and tends to progress towards neutral axis. Between the first and second peaks, main flexural crack propagates from the bottom tensile side of specimen to the upper side, the progress rate is restrained by fibre action and microshear crack occurrences spread out but with the positive bridging interaction effect of fibres, the second peak load can be reached. However, around and particularly after the second peak load, fibre pull-outs and ruptures cause perpetual decrease in load capacity and from this point, the specimen goes to the final failure point [6-8].

Acoustic emission (AE) is an effective and promising technique for macro synthetic fibre reinforced concrete in order to capture unclear points of damage progression and stiffness degradation of elements under increasing stresses. Fibre pull-out initiations and cracking progressions can be obtained and simultaneously characterized since AE method works in real-time. The variation of AE parameters is evaluated during loading and the acoustic activities of damage progress are able to be distinguished successfully.

A significant amount of research on the correlation of AE indices to the fracture properties has been carried out and the predictive relationships are obtained between AE waveform features and damage progression[9-13]. The most frequently used analysis are AE parameter based analysis, AE-SiGMA (AE-Simplified Green's functions for Moment Tensor Analysis) method and AE Rate Process Analysis[14-17]. The results show good agreement with the experimental ones. AE waveform features and changes in main parameters can be identified by the damage evolution and different energy transmission tendencies for tensile and shear cracks in the form of wave propagation. The studies have been conducted in different kinds of materials such as fibre polymer composites[18-19], concrete[20-22], steel fibre reinforced concrete[23-25] and FRP strengthened reinforced concrete structures[26-31]. To obtain meaningful information from AE signals, it is firstly necessary to have a working understanding of any changes in AE main parameters when fracture occurs. The drops and jumping increases in parameters such as average frequency, rise time or duration, etc. tells us the dynamic motion of deformations. There are some remarkable studies in the literature, which evaluate AE features in a more detailed manner for fibre concrete specimens[10,24,31]. The alterations of main parameters offer direct relationships with damage progression under increased loading[1,22,32-34].

There is also an alternative and practical method based on AE such as sentry function among recent AE studies[35-39]. Sentry function is the logarithmic ratio between strain energy and AE energy and the damage identification can be realized by help of variations in this function. The researches have been performed and the failure points can be characterized in the various types of concrete such as composite material strengthened reinforced concrete and fibre reinforced concrete[30,37,40-43].

The overall objective of this paper is to detect damage evolution and propagation in a more realistic manner under flexural loading in macro synthetic fibre reinforced concrete structures using AE technique. With this non-destructive technique, fractures can be determined in non-visible and non-accessible regions of systems. This enables us to correctly evaluate structural parameters of macro synthetic fibre reinforced concrete under increased loading, and real time assessments for structural systems. For this purpose, in the scope of this paper, AE response of MSFRC structures is observed with the experimental work that is reported in experimental study. AE parameters (Average frequency, RA (Rise time to Amplitude ratio) and Sentry functions) are evaluated for specimens and eventually, valuable results are directly captured so that AE characteristics are able to appropriately demonstrate the damage propagation for macro synthetic fibre reinforced concrete structures.

2 Materials and Methods

When material in a component deforms in response to loading, the deformation tends to relieve and the elastic energy stored will have been released in the stress field. Next, AE is produced at these sources as a pulse of energy, which travels through the material as an elastic wave. Emissions that continue during increased load levels indicate structurally significant defects even in inner and non-visible points in materials. AE wave propagation can be classified into four main modes that are longitudinal (P) waves, transverse (S) waves, surface (Rayleigh) waves and plate waves. In longitudinal waves, particles' motion is parallel to the direction propagation, while in transverse waves, particles' motion is perpendicular to the direction propagation. Surface waves such as Rayleigh and Love propagate on the surface of solids[1].

There is a close relation between damage structure and AE waveform features. Two typical crack modes

are considered as tensile and shear in order to describe the crack behaviour. When a tensile event occurs, the sides of cracks move away from each other. Since the nature of this deformation is the opposite movement of crack sides from each other, most of the energy transmitted in the form of longitudinal waves. Thus, shorter rise time, shorter duration and lower energy values are obtained with higher average frequencies. In a case of shear crack, the crack surfaces slide relative to each other and most of the energy is transmitted in favour of shear waves with small amount of longitudinal waves. Rise time, duration and energy of AE signals correspond to shear cracks, are higher than tensile ones when average frequency is lower than the tensile ones[1,44-46].

By calculating the RA(Rise time to amplitude ratio) value and the average frequency from equations (1) and (2), cracks can be grouped as shear cracks and tensile cracks based on the Japanese Codes JCMS-III B5706[47]. In tensile cracks, AE signals have higher average frequency and lower RA values due to the shorter rise time with higher amplitudes. However, since shear cracks are characterized by the transverse waves, AE signals have lower average frequency with higher RA values, as stated earlier.

□□ = (□□□□ □□□□ /□ℎ□ □□□□□□□□ □□□□□□□□□□) …(1)

□□□□□□□□ □□□□□□□□□□ = (□□ □□□□□□□□□ □□□□□□□ / □□□□□□□□□ □□□□□) …(2)

Sentry function is is expressed in terms of the logarithm of the ratio between the strain energy (E_S) and acoustic emission energy (E_{AE}), as given below:

$$(□) = \ln\left(\frac{E_S}{E_{AE}}\right) \quad \ldots(3)$$

This function f(x) is divided into five distinct areas as seen in Fig. 1; an increasing function PI(x), a sudden drop function PII(x), a constant function PIII(x), a decreasing function PIV(x) and a sometimes a button up function BU(x). Each region is associated with the specific stage in damage process. The sentry type PI(x) represents the strain energy storing phase when it is increasing. During the test, the ability of material to store energy reaches its limit, the material can recover itself and the AE cumulative energy significantly increases due to microcrack progression, hence the slope of the PI(x) function decreases seen as Fig 1. When a major failure occurs in the material, higher energy AE wave is produced and consequently, the stored mechanical energy is suddenly released. This explains the sudden drop in the function f(x) which is described by type function two, PII(x). After the failure occurrences, the slope of the next f(x) function tends to decrease until the material is no completely able to store its mechanical energy. At this stage the slope of the function reaches zero or below zero which are indicated by type III or IV function. Type III function explains the crack growth is stable but no any other fractures grow. Type IV, decreasing trend indicates that local existed failures propagate in an accelerated way and micro failures spread out to the whole the specimen. The button up(BU) function trend indicates that a strengthening mechanism takes place; this is not expected to be seen in any structures but in some types of steel fibre reinforced concrete structures[30,43].

The specimens were tested in three-point bending with AE measurements as seen from Figs 2 and 3. One reference concrete specimen(A0) and three MSF concrete specimens in 0.5%(A1), 1%(A2) and 1.5%(A3) volumetric ratios were prepared. Three-point bending test was conducted at a rate of 3 kg/s. The sizes of specimens were (150*150*600) mm. Concrete used for the specimen was a mixture of

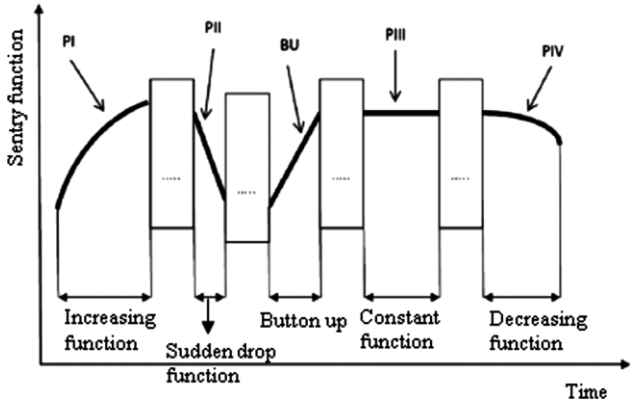

Fig. 1 — The sentry function phases.

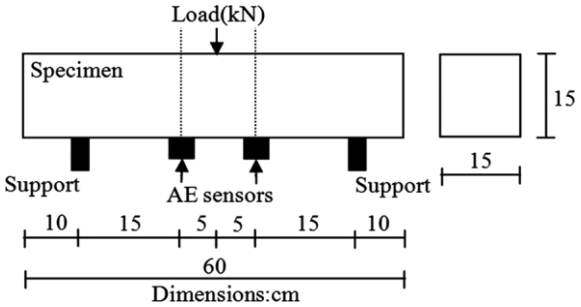

Fig. 2 — The schematic representation of three-point bending test setup.

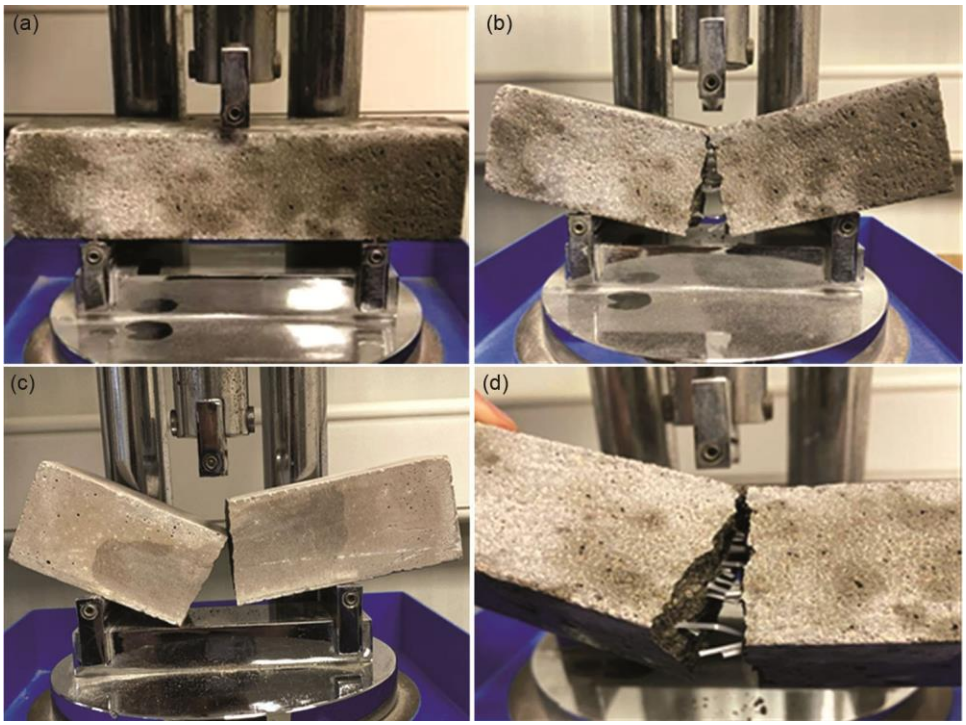

Fig. 3 — Three-point bending testing of specimens

Table 1 — The mechanical properties of macro synthetic fibres.

Length(l_f)	40 mm
Nominal diameter (d_f)	0.8 mm
Tensile strength(f_{tu})	400 MPa
Elongation at yield(ε)	20%
Modulus of elasticity(E)	4.3 GPa
Specific gravity(ρ)	0.9
Aspect ratio(l_f/d_f)	50

water, cement, 165 sand, and aggregate with the ratio of 0.68:1:2:3 by mass. The max. aggregate size was 16 mm. The mechanical properties of macro synthetic fibres are listed in Table 1. Three cylinder specimens (15cm*30cm) were cast and tested at the same time of the beam test to determine the compressive strength of concrete. The average compressive strength of 28 day concrete was 30 MPa.

Two AE broadband sensors (Pico, PAC) were attached to the bottom tensile side of the specimen to clearly evaluate crack progression. AE sensors of 200 kHz were attached to outer surface of concrete for AE measurements. AE device and sensors can be seen from Figure 4. Locations of sensors are added in Figure 2. A threshold level was set 40 dB and an 8 channel DiSP AE system(with frequency range 1 kHz-400 kHz and maximum amplitude 100 dB) was used to obtain AE data. Hit definition time(HDT) and Peak definition time(PDT) were consecutively 800 sec and 200 sec while Hit lockout time(HLT) was 200 sec. All the AE hits were used in the evaluations.

The frequency and intensity of the different Lamb wave modes, the signal attenuation, the sensor tuning, and the assessment of the source location performance were performed by means of a pencil lead break (PLB) test(Hsu Nielsen method)[20]. After the data acquisition and sensors setup, pencil leads with 0.3 mm were broken ten times and the emitted waveforms were captured by the sensors and recorded as digital signals. As defined in Fig. 4, the experimental setup was composed of main parts such as attached AE sensors, three-point bending setup, AE data acquisition system, computer and specimen.

3 Results and Discussion

The midspan load-deflection responses were obtained from three-point bending tests and presented in Figs (5-8). The load deflection curves generally consisted of three stages as pre-cracking, cracking and post-cracking phases.

In the first pre-cracking stage, almost linear behavior can be seen until the ultimate load for all specimens. The slope of the curve and the ultimate load capacity increased with the increase in fibre ratio 0.5%, 1% and 1.5%. External cracking initiation occurred with an increasing load, became visible and

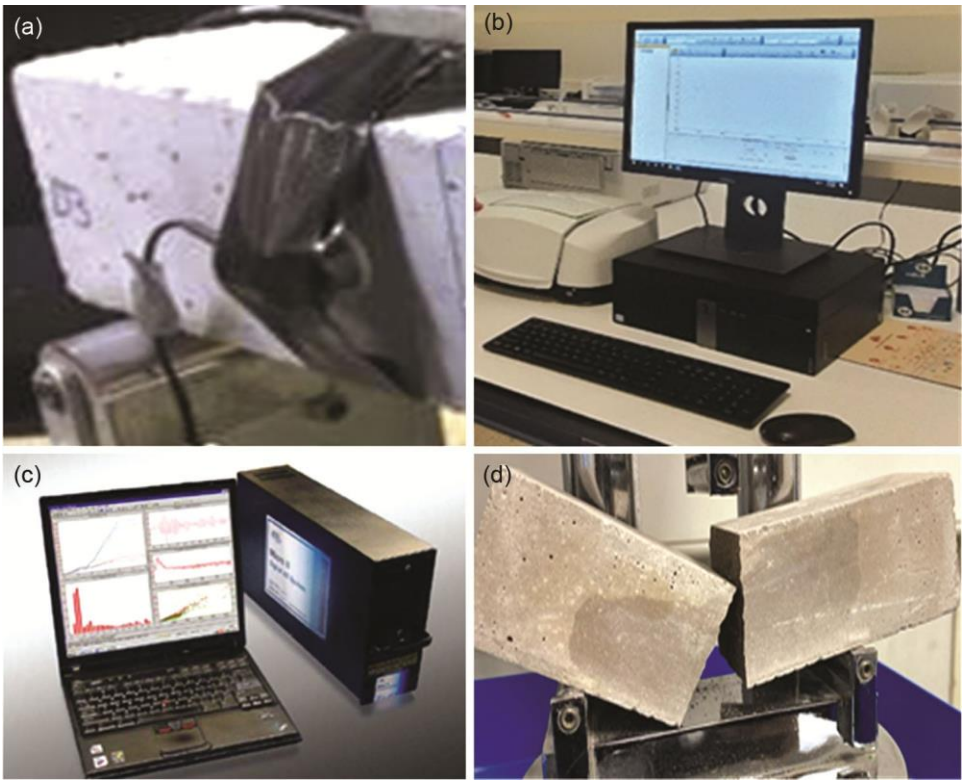

Fig. 4 — AE testing equipment.

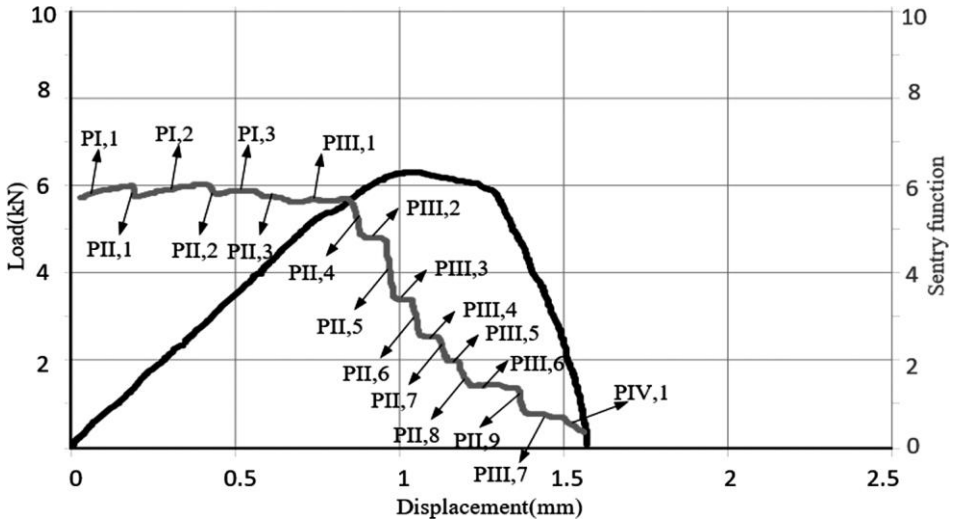

Fig. 5 — The sentry progression of reference concrete specimen(A0).

caused any inelastic processes for all specimens. The first peak load and corresponding midspan displacement values are 6218 N, 1.07 mm for A0, with the addition of macro synthetic fibres, 6325 N, 2.51 mm for A1; 7941 N, 2.38 mm for A2 and 8538 N, 2.35 mm for A3 with the increase in fibre ratio. It was so obvious that the fibre existence satisfactorily enhanced both the secant stiffness and toughness values of specimens improving their ductilities. The secant stiffnesses of A2 and A3 were higher than the other ones and furthermore, the toughness values were 3642 mJ for A0 while the higher values were consecutively obtained as 7886 mJ for A1, 10922 mJ for A2, 12342 mJ for A3. The post cracking stage has been monitored from the time that the midspan flexural crack propagated vertically through the

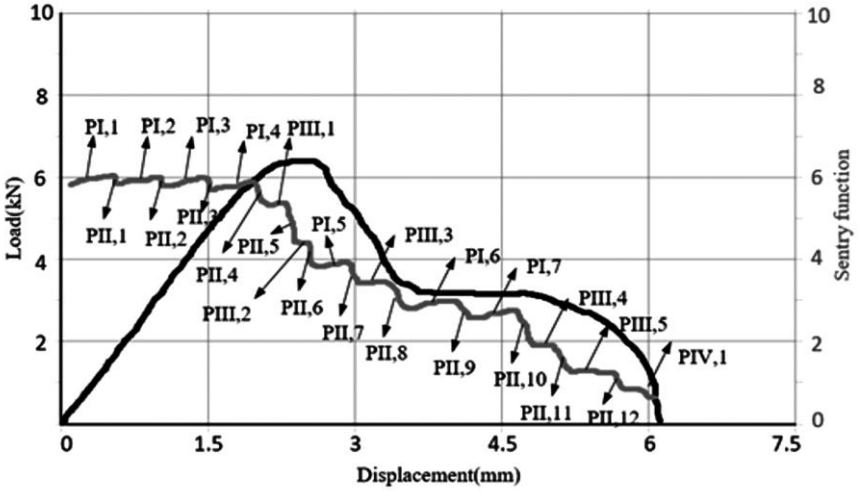

Fig. 6 — The sentry progression of MSFRC specimen(A1) with fibre ratio 0.5%.

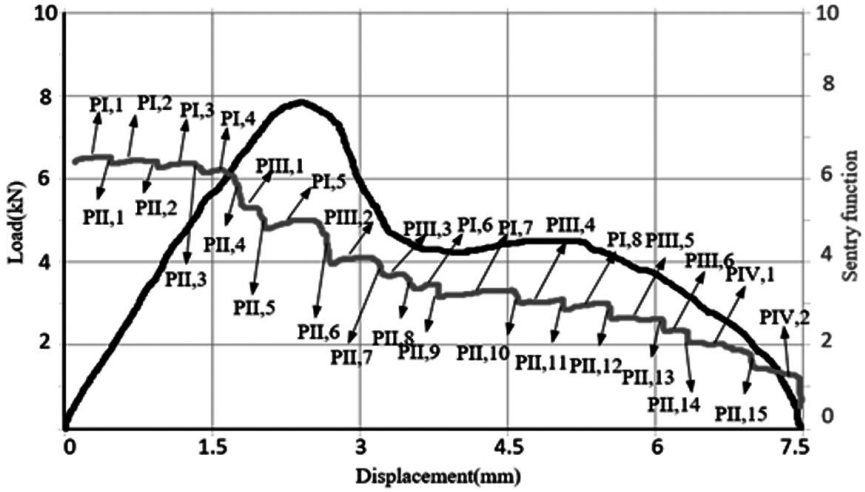

Fig. 7 — The sentry progression of MSFRC specimen(A2) with fibre ratio 1%.

height of beam until the failure. The load capacity decreased considerably with a stiffness reduction after first peak in load. The failure point was reached for concrete specimen in 1.56 mm midspan displacement. Reference concrete specimen(A0) had no second peak load. But, particularly, for A3 and A4, after reaching ultimate load and its consecutive local decrease, slight local increase in flexural load (second peak load) can be seen with the increase of deflection. The second peak load capacities and corresponding midspan displacements were 3386 N, 4.65 mm for A1; 4365 N, 5.06 mm for A2 and 5846 N, 5.62 mm for A3. However, this was not continuous, after second peak in flexural load; it went to the failure point. The same tendency was valid for A1 but the interpretation for the second peak in load was little bit difficult since the local increase was very smaller. The increase in fibre ratios resulted in an increased failure deflection capacities as 6.08 mm for A1, 7.51 mm for A2 and 7.58 mm for A3.

At the initial stages of loading, increasing functions (PI, n) were obtained with lower slopes for all specimens, the material recovered itself and kept its initial load bearing capacity, first sudden drop functions (PII,n) with very lower slopes followed but next, increasing functions can be monitored consecutively until the first peak load capacity of specimens. Whereas midspan cracking initiated and the first peak load was attained, first sudden drop functions with higher slopes were detected and became indicative sign of macro midspan cracks. Particularly for reference concrete specimen, constant functions(PIII,n) are monitored after sudden drops and decreasing function(PIV,1) indicated the final

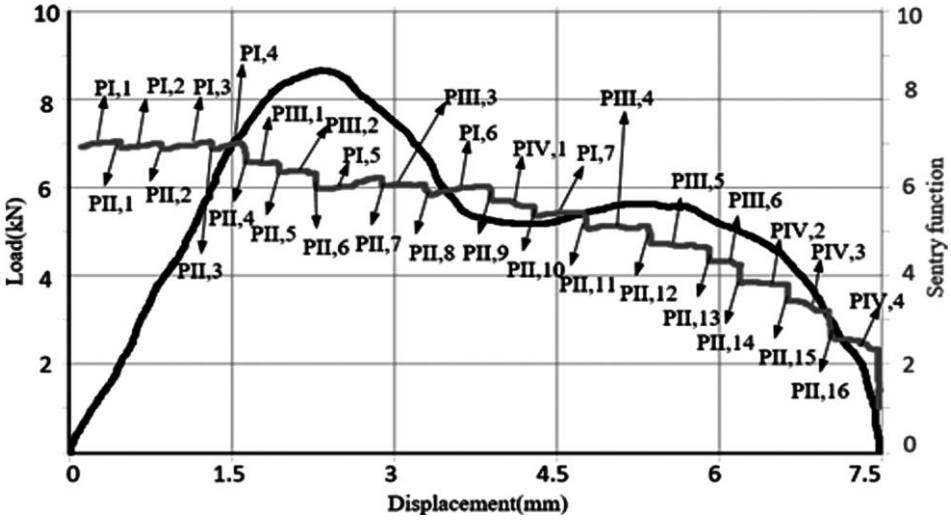

Fig. 8 — The sentry progression of MSFRC specimen(A3) with fibre ratio 1.5%

failure point of specimen. The slope value of decreasing function (PIV,a) was much higher in concrete due to its brittleness but with fibre addition, it tended to decrease in MSFRC specimens, as can be seen from Figs (6 & 8).

In the specimen(A1) with fibre ratio 0.5%, the local sharp sudden drops of sentry function in the region of ultimate load capacity were little bit softened in terms of their decreasing ratios however their numbers were increased according to concrete specimen(A0). Owing to fibre bridging mechanisms in concrete, after sudden drop functions(PII,n), specimen kept partially its ability to store its strain energy and increasing functions(PI,n) can be still obtained whereas there were always consecutive constant functions(PIII,n) after sudden drops in the reference concrete specimen. All the sudden drop functions clearly demonstrated midspan flexural cracking progression. First four sudden drops were related with midspan crack progression in the micro manner. PII,5 frankly displays the point at which the midspan flexural crack initiated and became visible. Three main increasing functions(PI,5; PI,6 and PI,7) and two main constant functions(PIII,1 and PIII,2) were monitored until second peak of load capacity. The second peak load capacity of specimen can be found out with sudden drop function(PII,10) because load capacity tended to decrease after this level due to the fact that the failure rate of material was higher before, the excessive progression of macro midspan crack brings to the sharpest sudden drop (PII,10) between the consecutive lower sudden drops and next, no increasing function(PI,n) was observed since the specimen cannot store its mechanical energy and released its AE energy. With the continuous decrease of load capacity, sentry function demonstrated constant functions (PIII,n) after sudden drops. The stored mechanical energy went down producing high energy AE waves. The decreasing function(PIV,1) indicated the point at which load capacity has been lost.

In the specimen(A2) with fibre ratio 1%, similarly with specimen 0.5%, increasing(PI,1, PI,2, PI,3 and PI,4) and consecutive drop functions(PII,1, PII,2, PII,3) were obtained until the first peak load capacity but increasing functions proved that the material was still capable of storing strain energy and local drops were related with midspan micro cracking occurrences. The load capacity of specimen reached to the ultimate value (7941 N) and after this level, tended to decrease due to the macro midspan crack initiation and progression. PII,4 was the indicative sign. Until the second peak of load capacity, crack progression was strained by help of fibre bridging mechanism, furthermore, more increasing functions (from PII,5 to PII,12) were obtained than the other specimens(A0 and A1) and constant functions (from PIII,1 to PIII,4) were monitored. Between the first peak and second peak loads, fibre addition provided that the following functions of sudden drops can be increasing functions(PI) which indicated micro damage occurrences were minimized and macro damage progression was slower owing to the improved ductility and strain energy storing capability. As the ductility of specimen was developed by help of fibre addition, flexural failure

progression can be restrained, the progressions of micro shear cracks were suppressed and the failure mechanism was dominated by main flexural crack propagation. Constant functions indicated that the midspan crack has been regularly grown, not at a rapidly rising rate or not induced by other microcrack formations. The lengths of constant functions were longer and the sharpness of local drops was softened. PII,12 was the sign of decrease in load capacity after second peak. After this point, with the continuous loss in the load capacity of specimen, as seen in Fig.7, sentry functions gave information about macro midspan crack progression and micro internal cracks development. The slopes of PII,13, PII,14 and PII,15 were lower than the other specimens'(A0 and A1). Owing to the fibre addition, macrocrack propagation rate had no jumps, being in a controlled manner. At the end of loading, PIV,1 and PIV,2 decreasing functions, smoother than A0 and A1, demonstrated more ductile response of specimen when it lost its load capacity.

The sentry progression of the specimen with fibre ratio 1.5% has the same tendency with specimens 0.5% and 1%, increasing (from PI,1 to PI,4) and consecutive drop functions (from PII,1 to PII,3) were obtained until the first peak load capacity, however, it was noteworthy that the rate of increasing functions were higher and slopes of local drops were much lower. The microcrack progression rate was much slower owing to the fibre addition. The first peak load capacity and the secant stiffness values were much higher than the other ones, after first peak load, PII,4 characterized the initiation of midspanmacrocrack formation. The slope of this sudden drop was much lower, midspan crack initiated but its propagation was strained by positive bridging effect of fibres although the identical load levels caused damage propagation in the other specimens. Between the first and second peak loads of specimen, the enhanced ductility and absorbed energy capacity enabled to small variations in values instead of jumps in sentry functions. Furthermore, increasing function(PI,5) can be even seen owing to the its strain storing ability, shorter sudden drops (from PII,4 to PII,12) indicated crack formations, PII,6, PII,9 and PII,11 were related with midspanmacrocrack progression through the height of beam whereas the others represented inner micro cracknucleations. The length of constant functions (from PIII,1 to PIII,5) were relatively longer than the values in the other specimens, this proved that the midspan crack propagation continued without accelerating in an uncontrolled manner and PIV,1 decreasing function has been lately met. Following this function, three shorter decreasing functions(PIV,2 to PIV,4) were also monitored without any sharper reductions and they represented how the load capacity has been lost in the domination of macro midspan crack progression with the enhanced ductility and absorbed energy capacity of specimen.

Average frequency(AF) and RA values are also valuable parameters which characterize the fracture processes and total failure mechanism of specimens under loading. For the specimens, the moving average trends of average frequency(red curve) and RA (green curve) were displayed in Figs (9-10). In Figures 9 and 10, F1 is the first peak load, F2 is the second peak load and F3 is the ultimate strain or failure point.

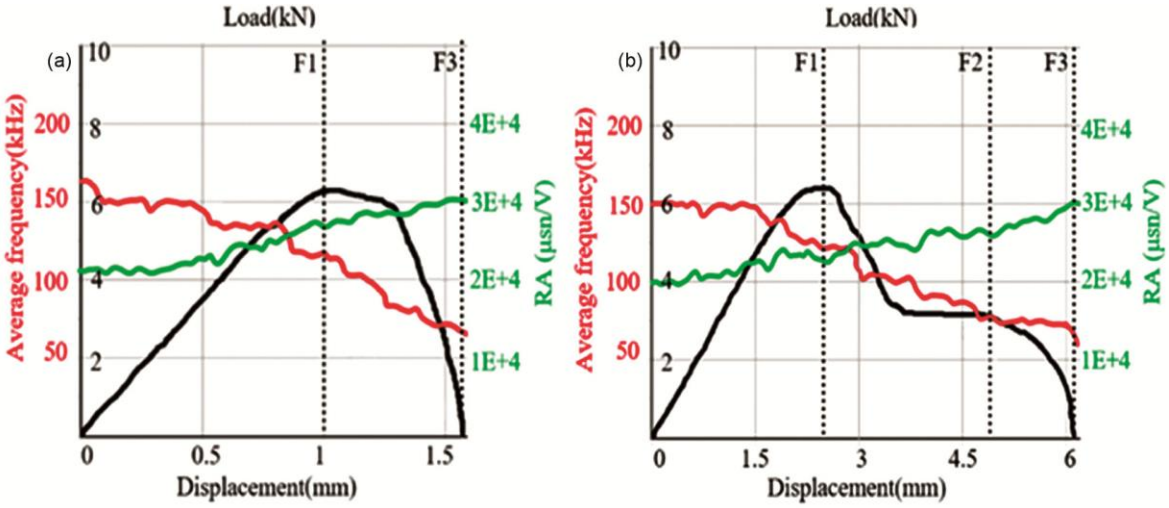

Fig. 9 — The average frequency(AF) and RA values for specimens (a) A0 and (b) A1.

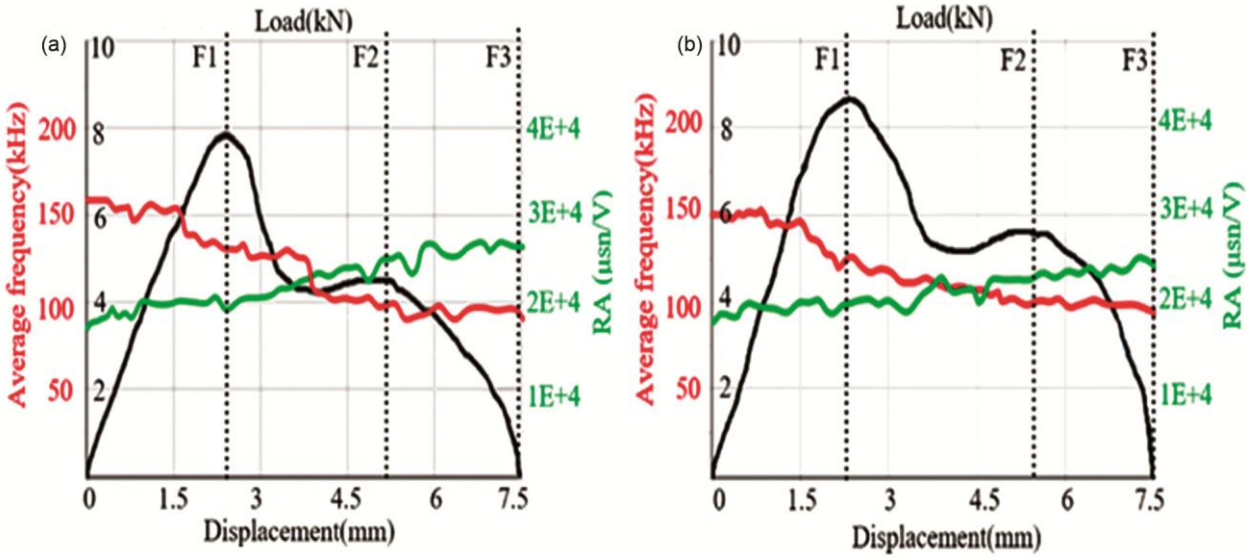

Fig. 10 — The average frequency(AF) and RA values for specimens (a) A2 and (b) A3.

As stated earlier, tensile cracks produce signals with relatively high frequency, while the shear type of cracks have lower values. Rise time, duration and energy of AE signals correspond to shear cracks, are higher than tensile ones when average frequency is lower than the tensile ones. Under three-point bending tests, cracking was initiated at the bottom surface of mid-beam due to the tensile loads (mode I). In reference concrete specimen, after the peak load, when shear microcracks(mode II) got gradually involved with tensile cracking events, the downshifts in average frequency and increases in RA were displayed. However, some alterations in curve were evaluated, shear micro cracks spread out to the inner section with the propagated flexural crack, the average frequency was decreased with drops while the tendency of RA was an increase. The drops were the signs of damage occurrences (flexural crack propagated and shear microcracks). For reference concrete specimen(A0), the sharper drops in average frequency and mini steep jumps in RA are more precise than the other specimens.

From the peak load, the concrete specimen demonstrated much more dramatic variations in average frequency and RA due to its brittleness, these points adequately estimated the damage nature and types.

In fibre concrete specimens, as the macro midspan flexural cracking development was extended to the top, the mechanism also began to form shear microcracks due to the fibre friction and pull out events occurrences. As can be seen in Figs 9 & 10, after first peak loads, first significant decreases in average frequency and short jumps in RA were noticeably seen for all specimens. But the shifts were softened as fibre ratio was increased in concrete owing to fibre bridging mechanism which made specimen more ductile. The shifts were matched for cracking events. Between the first peak and second peak loads, fibredebonding and pullout failures were responsible for sudden drops in average frequency and increases in RA for MSFRC specimens. As expected, the number of shifts was reduced with fibre addition. The events can be determined and simultaneously displayed by help of these shifts. Around the second peak, particularly for concrete specimen and MSFRC specimen that had 0.5% fibre content, sharper increases in RA clearly indicated the failure mechanism of fibres, exhibiting macro midspan cracking progression with strong microshear actions.

For specimen A1 (0.5% fibre content), increases in RA were also monitored as lower jumps with some fluctuations but they were the signs of the fracture processes. It was worth noting that major macro mid span cracking initiation was discriminated by the sharper drop in average frequency with jump in RA around the first peak load. The numbers of variations in values were increased between the first and second peak loads with the increased micro crackings. Like in the slopes of drops in sentry functions, the damage indicative shifts were more dramatic than the other fibre specimens. The decreasing rate is higher in average frequency and the first steep abrupt drop after

first peak load efficiently demonstrated the main flexural crack existence and progression. After the second peak load, with increasing AE events from micro crack occurrences and propagation of main macro crack, steep jumps in RA and sudden drops in average frequency were seen at the damage points. There were a lot of abrupt increases in RA particularly after second peak. This was primarily stem from new microshear cracks. Around and after second peak loads, variations in average frequency and RA matched well. As the system approached to the ultimate failure point, the regular decreases in mean average frequency and increases in RA acceleratingly continued without greater slopes and system failed.

For specimen A2(1%), as seen from Fig. 10, until the first peak load, variations in average frequency were more precise than in RA. However, for this region, it was noticed that decreasing rates in average frequency were lower than the other specimens A0 and A1 but the numbers were much more. Around the first peak load, the first abrupt decrease estimated the macro mid span crack initiation. After the first peak load, the increasing rates of RA were much higher and became clear damage indicators. It was interesting that there were some decreases after increases in RA around the second peak load. This pointed out that the fibre bridging capacity brought to second peak load, in other words, these decreases indicated the enhanced ductility behavior of specimen. Although the numbers of shifts in average frequency and RA were increased, the decreasing rates of average frequency were much slower. While the average frequency has been the good indicator for crack formations until the first peak load, RA estimations were more accurate around and after the second peak load. It can be added that the contribution of fibres weakened due to the inner pull-outs after the second peak load, the number of AE events was boosted until the failure point.

For specimen A3(1.5%), local alterations in RA and average frequency were limited in the whole parts of loading history. Similarly with specimen A2, the sudden drops in mean average frequencies were clearer and captured micro cracking points well. The rate of RA shifts was very smaller. Around the first peak load, average frequency characterized main midspan crack formation and initiation to propagate through the height of mid-beam as three consecutive sudden drops in average frequency. Between the first and second peak loads, like specimen A2, the numbers of shifts went up. RA demonstrated abrupt jumps in macro crack progression points while average frequency gave short decreases. Local decreases after each increase in RA were the important evidences of fibre bridging. After second peak load, fibre pullouts led to increase RA jumps while average frequency values included slight drops in cracking progression points. In other words, the final slight drops in average frequency were verified by the jumping increases in RA, macro crack progression points were mostly captured by help of RA jumps and after first peak load to the failure, micro shear crack occurrences were mostly discriminated with average frequency drops. The visual experimental observations confirmed these predictions stated with high accuracy.

4 Conclusion

AE indices as Average frequency, RA and Sentry functions are the most indicative and promising parameters in damage formation and progression.

For the sentry values, increasing functions(PI) have been initially met until the first peak load, Increasing function(PI) is attributed to the strain energy storing phase under loading while AE cumulative energy maintains lower level since no macro damage initiates. In MSFRC specimens, the increasing ratios between absorbed energy and AE energy were much greater as fibre ratios were increased from 0.5% to 1.5%. The following trends of increasing functions were sudden drops(PII) but the sharpest slopes were obtained in concrete. Sudden drops (PII) can be frankly explained by AE energy release produced from major failures versus decreasing capability of storing mechanical energy. Around the first peak load in all specimens, first sharpest sudden drops were the obvious signs of the onset of macro midspan cracking formations. As the fibre ratio in concrete was increased, the slopes of sudden drops were shortened and softened since the ductility and absorbed energy capacity of specimen was enhanced. Until the first peak load, micro tensile damage occurrences can be also distinguished by small decreases in average frequency and short increasing jumps in RA but fibre addition led to soften these alterations reducing microcracking. Around the first peak load, first significant drops in average frequency and steep increasing jumps in RA were captured. The midspan macro flexural cracking was formed and propagated towards the neutral axis. However, the inclined progression portions of cracking during its path and

newly microshear cracks occurrences were mainly responsible for the noticeable increasing jumps in RA and drops in average frequency.

Constant function(PIII) means that macrocracking steadily grows and no different failure mechanism is seen. Decreasing function(PIV) represents accelerated crack propagation while the strain storing energy of specimen drops off with greater AE energy release. After sudden drops, the shortest constant functions and decreasing functions with the highest slopes were noticed for concrete according to the MSFRC specimens. Between the first peak and second peak loads, fibre addition provides that the following functions of sudden drops can be increasing functions(PI), the longer constant functions and shorter decreasing functions with lower slopes have been also drawn attentions as fibre ratios went up from 0.5% to 1.5%. Microshear crack and macro midspan cracking formations caused local decreases in average frequency and jumps in RA. In specimens that had the highest fibre content 1% and 1.5%, these shifts were still visible but had shorter slopes. The second peaks were clearly discriminated by sentry portions and variations in AE indices, whereas the load-displacement curves remained insufficient. After second peak loads, for fibre concrete specimens, the numbers of AE activities were acceleratingly increased, the shifts explained microshear crack occurrences and upward progression of macrocrack. It was strongly emphasized that sentry progressions agreed well with the variations in average frequency and RA values.

Sentry function simultaneously provides the qualitative information about macro and microcrack formation and propagations in both external and internal sections while the accurate interpretation of average frequency and RA values ensures a clear understanding about the detection and identification of progressive failures in specimens.

Acknowledgments

The authors received no external funding for this research, gratefully acknowledge to the Engineering Labs of İzmir University of Economics for the experimental procedure and declared no conflict of interest.

References

1 Grosse U C, Ohtsu M, Aggelis D G, & Shiotani T, Acoustic Emission Testing: Basics for Research-Applications in Engineering (Springer-Verlag , Switzerland), 2nd Edition, ISBN: 9783030679354, 2022, p.752.
2 Alberti MG, Enfedaque A, & Gálvez JC,*Cem. Concr. Compos.*, 77 (2017) 29.
3 Amin A, Foster SJ, Gilbert RI, &Kaufmann W,*Cem. Concr. Compos*., 84(2017) 124.
4 Lerch, J O, Bester H L, Van Rooyen A S, Combrinck R, De Villiers W I, & Boshoff W P, Cem. Concr. Res., 103(2018) 130.
5 Bolat H, Şimşek O, Çullu M, Durmuş G, & Can Ö,*Composites Part B: Engineering*, 61(2014) 191.
6 Clarke T, Ghiji M, Fragomeni S, & Guerrieri M, *Struct. Concr*., 24(2023) 1244.
7 Nana W S A, Tran H V, Goubin T, Kubisztal G, Bennani A, Bui T T, Cardia G, & Limam A, Structures, 32(2021) 1271.
8 Guerini V, Conforti A, Plizzari G, & Kawashima S, Fibers, 6(2018) 47.
9 Aggelis D G., Mech. Res. Commun., 38(2011) 153.
10 Aggelis D G, Soulioti D V, Barkoula N M, Paipetis A S, & Matikas T E, Cem. Concr. Compos., 34(2011) 62.
11 Grosse U C & Finck F (2006), Cem. Concr. Compos., 28(2006) 330.
12 Rucka M, Knak M, & Nitka M, *Eng. Fract. Mech*., 293(2023) 109718.
13 Zhang X, Jin J, Jiang J, Wang C, Yang Y, Li Y, Liu K, Chen G, Bo W, Sun H, & Liu T, *Opt. Lasers Eng.,* 171(2023) 107823.
14 Botvina L R, Bolotnikov A I, Sinev I O, &Beletsky E N, Eng. Fract. Mech., 292 (2023) 109635.
15 Lian S, Zheng K, Zhao Y, Bi J, Wang C, & Huang Y S, Constr. Build. Mater., 362(2023) 129789.
16 Shigeishi M & Ohtsu M, *Constr. Build. Mater*., 15(2001) 311.
17 Yu X, Montrésor S, Bentahar M, &Mechri C, *Appl. Acoust*., 211(2023) 109533.
18 Barile C, Casavola C, Pappalettera G, & Kannan V P, Compos. Struct., 292(2022) 115629.
19 Brunner A J, Constr. Build. Mater., 173(2018) 629 637.
20 Aggelis D G, Soulioti D V, Sapouridis N, Barkoula N M, Paipetis A S, & Matikas, T E, Constr. Build. Mater., 25(2011) 4126.
21 Khrishnaa S, Veerendar C, Prakash S S, & Kawasaki Y (2023), Constr. Build. Mater., 402(2023) 132983.
22 Ohtsu M, *Adv. Mater. Res*., 13-14(2010) 183.
23 Ashraf S & Rucka M, Constr. Build. Mater., 395(2023) 132306.
24 Soulioti D, Barkoula N M, Paipetis A, Matikas T E, Shiotani T, & Aggelis D G, Constr. Build. Mater., 23(2009) 3532.
25 Tayfur S, Alver N, Abdi S, Saatcı S, & Ghiami A, Eng. Fract. Mech., 194 (2018) 73.
26 Alver N, Tanarslan H M, Sülün Ö Y, Ercan E, Karcılı M, Selman E, & Ohno K, Cons. Build. Mater., 67(2014) 146.
27 Alver N, Tanarslan H M, & Tayfur S., J. Infrastruct. Syst., 23(2016) B4016002.
28 Ma G & Li H, *Constr. Build. Mater*., 144(2017) 86.
29 Liu K, Wulan T, Yao Y, Bian M & Bao Y, *Eng. Struct*., 300(2024) 117228.
30 Selman E, Ghiami A, & Alver N, *Constr. Build. Mater*., 95(2015) 832.
31 Tayfur S, Alver N, Tanarslan H M, & Ercan E, Constr. Build. Mater., 164(2018) 864.
32 Hu S, Lu J, & Xiao F, *Constr Build Mater*, 47(2013) 1249.
33 Ohno K & Ohtsu M, *Constr Build Mater*, 24(2010) 2339.
34 Zhang F, Yang Y, Fennis S, & Hendriks M, *Constr Build Mater*, 318(2022) 126163.

35 Barile C, Casavola C, Pappalettera G, & Kannan V P, Composites Part B: Engineering, 178(2019) 107469.
36 Davijani A A B, Hajikhani M, & Ahmadi M, Mater. Des, 32(2011) 3059.
37 Fotouhi M & Najafabadi M A, J. Thermoplast. Compos. Mater., 29(2016), 519.
38 Oskouei A R, Zucchelli A, Ahmadi M, & Minak G, Mater. Des., 32(2011), 1444.
39 Zhou W, Zhang P, & Zhang Y, Appl. Sci., 8(2018), 22-65.
40 Kumar C S, Arumugam V, & Santulli C, Composites Part B: Engineering, 111(2017) 165.
41 Monti A, El Mahi A, Jendli Z, & Guillaumat L, *Composites Part A: Applied Science and Manufacturing*, 90(2016) 100.
42 Sagar R V & Basu D J (2022), Nondestruct. Test. Eval., 38(2022) 612.
43 Saeedifar M & Zarouchas D, Composites Part B: Engineering, 195(2020) 108039.
44 Aggelis D G, Shiotani T, Momoki S, & Hirama A, ACI Materials Journal, 106 (2019) 509.
45 Aggelis D G, Shiotani T, & Terazawa M, J. Eng. Mech., 136(2010), 906.
46 Aggelis D G, Mpalaskas A C, Ntalakas D, & Matikas T E, Constr. Build. Mater., 35(2012) 183 190.
47 JCMS-IIIB5706, Monitoring method for active cracks in concrete by acoustic emission. Japan Construction Material Standards IIIB5706, 2003.